

AN EXPERIMENTAL SETUP FOR COMBINED WAVE-CURRENT FLOW INTERACTING AT A RIGHT ANGLE OVER A PLANE BEACH

MASSIMILIANO MARINO^(*), CARLA FARACI^(**) & ROSARIA ESTER MUSUMECI^(*)

^(*)University of Catania – Department of Civil Engineering and Architecture – Via Santa Sofia, 46 – 95123, Catania, Italy

^(**)University of Messina – Department of Engineering – C.da Di Dio 98166, Messina, Italy

Corresponding author: ms.marino@unict.it

EXTENDED ABSTRACT

Onde e correnti sono spesso presenti simultaneamente in zona costiera. La loro interazione dà luogo ad un complesso campo di moto idrodinamico, il quale governa importanti processi costieri e.g. trasporto solido. Lungo la costa tale campo di moto è ulteriormente complicato dall'interazione con il fondale, il quale può essere fisso, erodibile, inclinato o presentare forme di fondo. Sebbene siano stati compiuti grandi progressi nello studio dell'interazione onde-correnti e nello sviluppo dei relativi modelli teorici, la conoscenza del fenomeno presenta ancora delle criticità importanti. Innanzitutto, la maggior parte dei dati sperimentali esistenti provengono da esperimenti sull'interazione fra onde e correnti co-lineari, ovvero aventi la stessa direzione, sebbene l'angolo di attacco fra onde e correnti avvenga in zona costiera prevalentemente con un angolo ortogonale o quasi ortogonale. La mancanza di dati nelle suddette condizioni è probabilmente dovuta a difficoltà connesse alla modellazione fisica e alla mancanza di apparati di laboratorio adeguati alla riproduzione di questo particolare campo di moto. Ciò ha fatto sì che i modelli teorici esistenti siano stati validati prevalentemente su esperimenti co-lineari, malgrado studi recenti mostrino come questo abbia determinato una insensibilità direzionale ed una non corretta ricostruzione degli sforzi tangenziali al fondo di tali modelli. Inoltre, i pochi esperimenti esistenti sono prevalentemente su fondo piano, dunque gli effetti non lineari determinati dalla propagazione del moto ondoso su un fondale con profilo inclinato (e.g., shoaling) su una corrente diretta ortogonalmente non sono stati studiati approfonditamente in letteratura.

Nel presente lavoro è stato condotto uno studio sperimentale sull'interazione ortogonale fra onde e correnti su fondo inclinato. Il lavoro è incentrato sulla caratterizzazione idrodinamica del setup sperimentale. Una serie di esperimenti è stata effettuata all'interno di una vasca sperimentale, dove mediante un generatore di onde e un sistema di ricircolo delle correnti è possibile dar luogo alla contemporanea presenza di onde e correnti interagenti ad angolo retto. Sono stati effettuati esperimenti sia in condizioni di sola corrente che di onde più correnti. Il moto ondoso e la corrente interagiscono in corrispondenza di un fondo fisso liscio con pendenza 1:25. Un moto oscillatorio regolare con altezza d'onda $H = 0.01$ m e periodo $T = 1.0$ s è stato sovrapposto ad una corrente con velocità media $U = 0.11$ m/s. Sono stati condotti 19 test, 14 dei quali in condizione di sola corrente e 5 in condizione di onde più correnti. La sopraelevazione d'onda e le velocità sono state misurate, rispettivamente, mediante sonde resistive e velocimetri acustici ad effetto Doppler. I velocimetri sono stati posizionati all'interno dell'area di acquisizione al fine di caratterizzare spazialmente il campo di moto. Nello specifico, sono state riprodotte tre disposizioni geometriche della strumentazione di misura: con un array lineare in direzione della corrente, con un array lineare in direzione delle onde, a croce in entrambe le direzioni.

In presenza di sola corrente, i risultati dei profili di velocità media mostrano che all'interno del setup sperimentale è possibile riprodurre una corrente soddisfacentemente ortogonale rispetto alla direzione del moto ondoso, sebbene all'allontanarsi dall'asse di mezzera della sezione di ingresso e di uscita della corrente questa subisce un effetto di deviazione nella direzione del moto ondoso. Questo suggerisce la presenza di regioni di ricircolo, le quali all'allontanarsi dalla regione di ingresso/uscita della corrente inducono una deviazione del flusso in direzione ortogonale rispetto alla direzione prevista. I profili di velocità mostrano inoltre la presenza di un moto medio verticale in direzione normale al fondo. Questo può essere dovuto ad un rallentamento della corrente in prossimità della sezione di uscita. In presenza di onde sovrapposte alla corrente, i risultati dei profili di velocità media mostrano un aumento di velocità della corrente per effetto della sovrapposizione del moto ondoso. Tale dato suggerisce la presenza di un trasferimento di quantità di moto media nella direzione della corrente per effetto del moto oscillatorio. L'incremento di velocità è maggiore a profondità relativamente minori, ed è tale da ridurre l'effetto di richiamo delle regioni di ricircolo.

ABSTRACT

In the present work an investigation on combined wave-current orthogonal flow over a planar beach is presented. A series of tests have been carried out in an experimental tank, in which a wavemaker coupled with a flow recirculation system allows the superposition of an oscillatory flow over an orthogonal steady current. Waves and current interact over a fixed smooth bed with a 1:25 sloping profile. Current only and wave plus current tests have been performed, during which surface elevation and velocity profiles measurements have been recovered. Velocity measurements have been carried out at different positions in the tank in order to investigate effects on the velocity profile determined by presence of the sloping bottom at different depths. Results of current only tests showed that a satisfactory steady current is achieved within the tank, although presence of a minor recirculation effect determines a mean flow to arise in the direction orthogonal to the current. Superposition of waves determines a mean momentum transfer on current, which results in an increased current velocity and a reduction of the recirculation effect.

KEYWORDS: *nonlinear waves, wave-current interaction, nearshore current, sediment transport*

INTRODUCTION

Waves and currents are generally simultaneously present in coastal and estuarine environments (SVENDSEN, 2006; STANCANELLI *et alii*, 2018; VIVIANO *et alii*, 2018, STANCANELLI *et alii*, 2020). The hydrodynamics of wave-current combined flow drives important coastal processes, such as sediment transport. A fairly amount of experimental investigations on wave-current interaction (WCI) has been carried out in the last decades with waves and current propagating in the same or opposite directions (KEMP & SIMONS, 1983; MATHISEN & MADSEN, 1996; LODAHL *et alii*, 1998) or with currents generated by wave breaking (SANCHO *et alii*, 2001; DE SERIO & MOSSA, 2013). Although in the near-shore WCI usually occurs with a near-orthogonal angle of attack, experimental data on WCI at a right angle are relatively limited, probably due to difficulties in the physical modeling. MUSUMECI *et alii* (2006) investigated orthogonal WCI over sand and gravel bottoms in a 3D tank, showing that an oscillatory flow out of phase with respect to the wave velocity is observed in the current direction in the presence of the combined flow. FARACI *et alii* (2008) investigated combined waves and currents over flat bed and fixed ripples through numerical and laboratory tests. Results showed that presence of ripples act as a macroroughness, inducing turbulence to intensify and current apparent roughness to increase. FERNANDO *et alii* (2011) carried out experiments of WCI at a right angle in a wave basin over movable bed, from which bed shear stresses

have been recovered, and results compared with theoretical models of wave-current combined flow nonlinear interaction. Results showed that for the larger wave heights none of the models has been able to reconstruct properly the observed velocity profile, whereas for smaller wave heights most of the models are in good agreement with the observations. FARACI *et alii* (2018) gathered near-bed velocity statistics of WCI at a right angle over different roughness elements: sand, gravel and ripples. Probability density function of near-bed velocities showed a Gaussian distribution for current only case, whereas a double peak distribution is observed in the combined flow. Characteristics of the double peak is strictly related to the wave kinematics such as wave steepness and relative water depth. An investigation on turbulent flow was also carried out, showing an alteration of near-bed high order velocity statistics, such as skewness and kurtosis, exerted by oscillatory flow on current. Slight differences between the different bed roughnesses have been observed. LIM & MADSEN (2016) investigated WCI with different angles of attack (60°, 90° and 120°) over a ceramic marble bottom, and compared the velocity profile at the bottom boundary layer with the one modeled by the GRANT & MADSEN (1979) model (GM). Results showed that, when as the angle between wave and current directions increases, the GM model tend to over-predict wave influence on current. Moreover, presence of nonlinear components in the wave motion may induce a veering of the current from its main direction due to turbulence asymmetry.

Despite the amount of effort in investigating WCI, the phenomenon is not yet well understood and some critical issues remain. First, experimental data of WCI at a right angle are scarce, thus most of the existing models have been validated by means of collinear WCI experimental data. This resulted in a directional insensitivity and an incorrect estimation of bottom shear stresses of these models. Moreover, presence of coastal hydrodynamics processes related to a depth varying bottom which induce large nonlinearities (MARINO *et alii*, 2018), have not been investigated extensively in the context of WCI at a right angle.

The present work investigates WCI at a right angle over a sloping bed by means of a laboratory investigation in a wave tank. The work focuses on the issues encountered in the development of the experimental setup, and on the correct reconstruction of the WCI hydrodynamics over a sloping profile in a laboratory environment, about which few studies exist (MARINO *et alii*, 2020). The flow is analyzed at different locations of the tank with different water depth, in order to observe how the flow field is altered by the presence of the slope at different depths. Surface elevation and 3D velocity measurements have been recovered by means of resistive wave gauges and an Acoustic Doppler Velocimeter respectively.

The paper is organized as follows: in the first section the experimental setup, plan and procedure are described in detail along with the velocity data treatment, in the second section results from the velocity data analysis are discussed. A concluding section closes the work.

EXPERIMENTS

An experimental campaign in a wave tank (18.00 x 3.40 x 1.00 m) at the Hydraulics Laboratory of the University of Catania (IT) has been carried out. The top view of the experimental tank is shown in Figure 1.

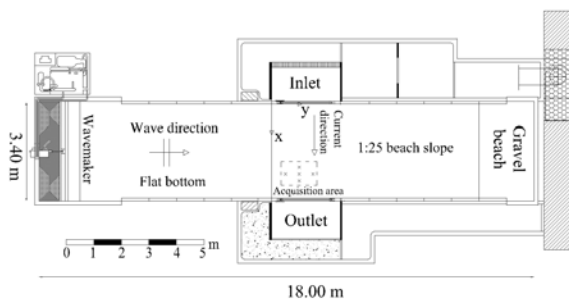


Fig. 1 - Experimental wave-current tank.

At the offshore end of the tank, a flap-type wavemaker allows the generation of regular waves; at the onshore end a coarse material beach acts as a wave reflection passive absorber. A recirculation system generates a steady current, which crosses the wave field at a right angle. The current is conveyed into the tank by an 11.0 kW submerged pump, with a maximum discharge of 0.25 m³/s; it flows within a series of channels and comb filters in order to dampen turbulence. The flow enters the flume crossing through a 2.5 m wide current inlet and flows out through a 2.5 m outlet mirrored to the inlet section.

Waves are generated over a horizontal bottom (water depth $h = 0.30$ m) and then shoal on a 1:25 fixed planar beach. Surface elevation is measured by means of 5 resistive wave gauges (WG), with one WG located in the proximity of the wave maker, and 4 WG right behind the start of the slope; wave reflection is computed through the 4-probes method by FARACI *et alii* (2014). Velocity measurements are gathered by means of a Nortek Vectrino Acoustic Doppler velocimeter (ADV), which measured velocities u^* , v^* and w^* in the x (current-), y (wave-) and z (vertical upward-) direction respectively, where the * denote dimensional quantity. The resolution of the ADV is 0.001 m/s, the accuracy is $\pm 0.5\%$ of the measured value. Sampling frequency is 50 Hz for the WGs and 100 Hz for the ADVs.

Experiments in the presence of current only (CO) and waves plus current (WC) have been carried out, for a total of 19 tests.

	Test	Regime	x [m]	y [m]	h [m]	H [m]	T [s]
Line (x)	1	CO	2.00	1.00	0.26	-	-
	2	CO	2.25	1.00	0.26	-	-
	3	CO	2.50	1.00	0.26	-	-
	4	CO	2.75	1.00	0.26	-	-
	5	CO	3.00	1.00	0.26	-	-
Line (y)	6	CO	2.50	0.50	0.28	-	-
	7	CO	2.50	1.00	0.26	-	-
	8	CO	2.50	1.50	0.24	-	-
	9	CO	2.50	2.00	0.22	-	-
	Cross	10	CO	2.25	1.00	0.26	-
11		CO	2.50	1.50	0.24	-	-
12		CO	2.50	1.00	0.26	-	-
13		CO	2.50	0.50	0.28	-	-
14		CO	2.75	1.00	0.26	-	-
Cross	15	WC	2.25	1.00	0.26	0.085	1.0
	16	WC	2.50	1.50	0.26	0.085	1.0
	17	WC	2.50	1.00	0.26	0.085	1.0
	18	WC	2.50	1.50	0.24	0.085	1.0
	19	WC	2.75	1.00	0.28	0.085	1.0

Tab. 1 - Experimental plan: number of tests, wave-current regime, ADV positions and patterns and wave conditions.

Mean current velocity U is equal to 0.11 m/s for all tests, regular wave characteristics are: wave height $H = 0.085$ m and wave period $T = 1.0$ s. The list of the experiments is shown in Table 1. Test duration is 10 minutes.

For every test the ADV is deployed in a different position in the tank in order to follow a specific pattern. In tests 1-5 the flow regime is CO and velocity measurement positions follow a line pattern parallel to the x direction, thus every test has a different x ($= 2.00 \div 3.00$ m) and same y ($= 1.00$ m) and h ($= 0.26$ m). In tests 6 - 9 the wave-current regime is CO, velocity measurement positions are chosen in order to follow a line pattern parallel to the y direction, thus every position have a different y ($= 0.50 \div 2.00$ m) and consequently a different h ($= 0.22 \div 0.28$ m), as y is the direction of the increasing slope, and same x ($= 2.50$ m).

In tests 10-14 the regime is CO and velocity measurement positions are located as to follow a cross pattern, with a central position ($x = 2.50$ m and $y = 1.00$ m), two positions with same y but different x ($x = 2.50 \pm 0.25$ m, $y = 1.00$ m) and two positions with same x but different y ($x = 2.50$ m, $y = 1.00 \pm 0.50$ m). In WC tests 15-19 the ADV positions are the same of tests 10 - 14, with a wave height $H = 0.01$ m and a wave period T of 1.0 s. ADV positions during the tests are reported in Table 1.

Velocity data are treated in order to remove spikes and outliers determined by electrical noise or temporary lack of seeding particles that prevents acoustic reflection to occur. Signal with signal-to-noise ratio less than 10 and correlation less than 70% are removed and then replaced by means of a cubic polynomial fitting of the remaining local data. Velocity measurements are treated in order to remove spikes with GORING & NIKORA (2002) phase-

space despiking method, which are removed and then replaced by means of cubic polynomial fitting. Average amount of replaced data is 15% ($\pm 4\%$) of the original time series. Regarding wave plus current experiments, velocity and wave height measurements are phase-averaged in order to obtain phase-averaged quantities of interest and to carry out a phase analysis.

The number of wave cycles used within the computation of the ensemble averaged wave is 600, fairly larger than the 50 wave cycles minimum recommended by SLEATH (1987) to compute phase-averaged wave quantities. Figure 2 shows the phase-averaged wave surface elevation for Test 17 measured in correspondence of the flat bottom ($x = 1.70$ m, $y = -1.00$ m).

The maximum standard deviation is observed in correspondence of the wave crest and is equal to ± 0.0058 m, corresponding to 6% of the wave height. Average standard deviation at the wave crest for all the tests is 6%, with a maximum of 15% for test 19. Wave peak period satisfactorily corresponds to the target of 1.0 s, with an average deviation of 2% and a maximum of 4% for test 19. Parameters h/gT^2 and H/gT^2 have been computed in order to characterize the generated wave field (DEAN, 1970). In correspondence of the flat bottom ($h = 0.3$ m), average shallowness parameter for all tests is 0.030 whereas average nonlinear parameter is 0.012, therefore generated waves can be considered highly nonlinear waves in intermediate depth, in the range of validity of Stokes 5th order wave theory, relatively close to the wave breaking limit ($H/h \approx 0.8$). In the acquisition area shallowness parameter ranges from 0.028 to 0.024 as depth decreases along the bed slope, therefore wave shoaling is expected, although never reaching the wave breaking limit.

RESULTS

In the present section the results of the time-averaged velocity profile data analysis are presented and discussed. Velocity profile

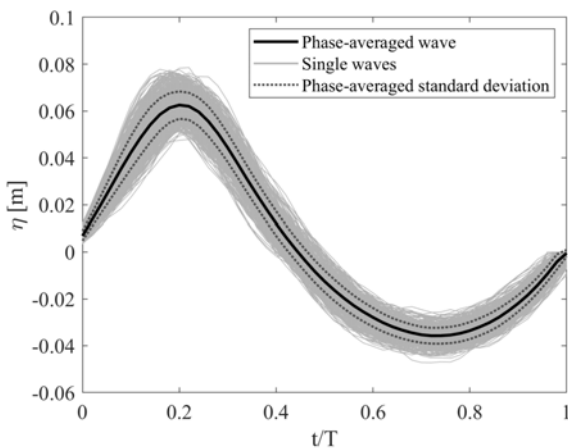


Fig. 2 - Phase-averaged wave surface elevation for test 17.

analysis is an indirect technique to observe flow resistance determined by bottom shear stresses, which computation is extremely important in the study of sediment transport (MUSUMECI *et alii*, 2018) and the characterization of the hydrodynamic flow field in general. Figure 3a shows the dimensionless time-averaged $u = \bar{u}/U$ and $v = \bar{v}/U$ velocity profiles, where \bar{u} and \bar{v} are the time - averaged dimensional velocities in the current and wave direction respectively for tests 1 - 5 (CO), Figure 3b shows the three-dimensional representation of u , v and w for the same tests. Within these tests y remain constant ($y = 1.00$ m) whereas x is different ($x = 2.25 \div 2.75$ m), thus the positions of the ADV are aligned in the x direction, thus the local depth h is constant and is equal to 0.26 m.

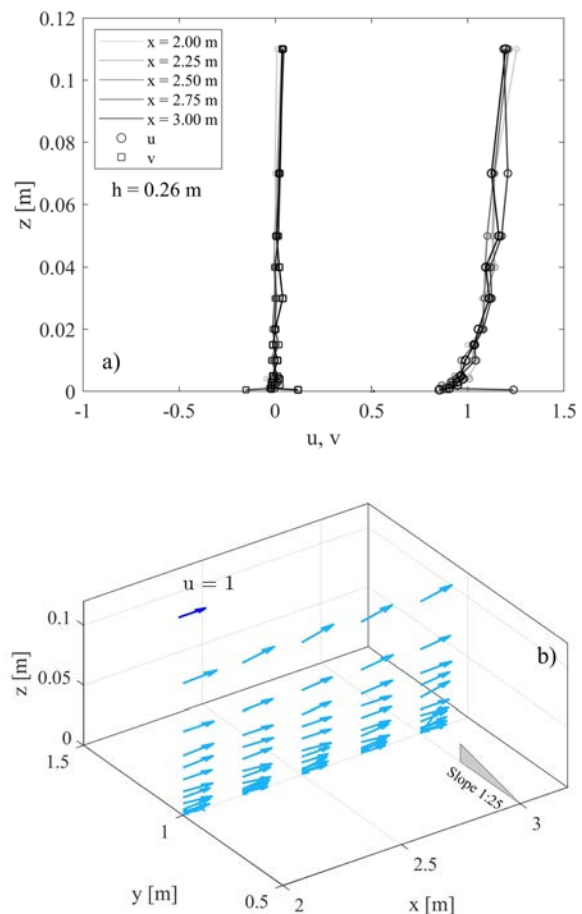


Fig. 3 - Dimensionless time-averaged velocity vertical profiles in the current direction (u , circles) and in the wave direction (v , squares) with same y and different x (shades of grey) (a), and the three-dimensional representation of u , v and w with their position in the tank (b) for tests 1-5 (current only). Local depth $h = 0.26$ for all tests.

Figure 3a shows that along $y = 1.00$ m all the velocity profiles present a quite similar behavior, for both u and v . No noticeable mean flow in the y direction is observed, showing that a steady unidirectional current in the x direction is satisfactorily achieved. Velocity peaks are observed in the proximity of the bed for both u and v . Here, likely, the sampling volume of the ADV partially crosses the bottom plane, in this case the velocity measurement is considered unreliable. Figure 3b shows a slight constant mean flow in the upward z direction. This could be explained by the presence of a slight tilt, i.e. an incorrect inclination of the velocimeter, which may be not perfectly vertical and determine the current flow to be read along the z direction, thus the ADV is measuring a component of u in w . Another possible explanation could be that the proximity of the outlet may determine an effect

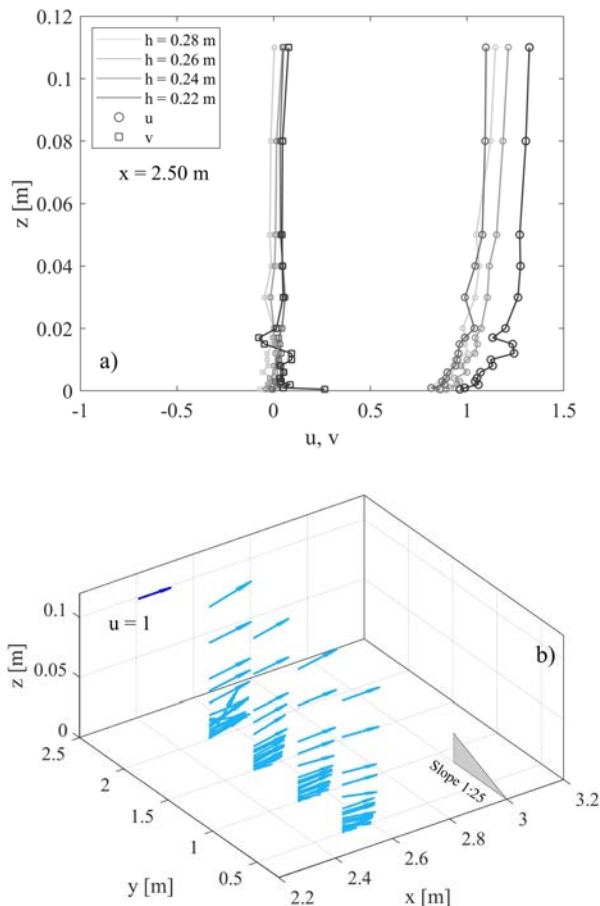


Fig. 4 - Dimensionless time-averaged velocity vertical profiles in the current direction (u , circles) and in the wave direction (v , squares) with same y and different x (shades of grey) (a), and the three-dimensional representation of u , v and w with their position in the tank (b) for tests 6-9 (current only). Local depth h ranges from 0.22 m to 0.28 m.

induced by the presence of a slower current downstream of the outlet, prompting the flow to be partly conveyed upward.

Figure 4a shows the time-averaged u and v velocity profiles, while Figure 4b shows the three-dimensional representation of u , v and w for tests 6-9 (current only). Within these tests x remain constant ($x = 2.50$ m) while y is different ($y = 2.00 \div 3.00$ m), thus the positions of the ADV are aligned in the current direction. Local depth h ranges from 0.28 m (test 6) to 0.22 m (test 9).

Figure 4a shows that as the local depth decreases in the y direction, velocity in the current direction gradually increases along the water column. Indeed, as the height of the inflow / outflow section decreases in the y direction, velocity increases in the y direction to preserve mass continuity. However, profile at $h = 0.24$ m seems not to follow this behavior, showing a velocity decrease with respect to the profile at $h = 0.26$ m. This could be due to the presence of a recirculation flow in the shoreward direction, although no mean flow in the y direction is observed at the same position. Figure 4b shows the presence of the mean upward flow as already observed in Figure 3b.

Figure 5a shows the dimensionless time-averaged u and v velocity profiles, while Figure 5b reports the top-view of the 3D velocity field for tests 10-14 (current only). Within these tests the ADV positions follow a cross pattern, as described in Section 2. In Figure 5a the marker indicates the y coordinate, the line type indicates the x coordinate. Figure 5b shows a different perspective (top view) with respect to the one shown in Figure 3b and 4b. In the cross pattern, the position closer to the wavemaker is also called “seaward position” ($y = 0.50$ m, $h = 0.28$ m), the position closer to the gravel beach ($y = 1.50$ m, $h = 0.24$ m) is called “shoreward position”, the three positions in the middle ($y = 1.00$ m, $h = 0.26$ m) are called “central positions”.

Figure 5a shows that the u profiles at the central positions (square marker), in comparison with the seaward position (downward triangle marker, dashed line), show a larger depth-averaged velocity determined by the continuity effect already observed in Figure 4a. Figure 5a also shows that the shoreward u profile (upward triangle marker, dashed line) do not follow this behavior, showing instead a decreased velocity. As observed in tests 6-9, the presence of the recirculation region may determine the flow to be conveyed in the shoreward direction. Velocity profiles of v in Figure 5a show the presence of a mean flow at the shoreward position along the wave direction, although only for the lower part of the profile. Figure 5b shows the effect of the recirculation at the shoreward position, although less visible than in the velocity profiles.

Figure 6a shows the time-averaged u and v velocity profiles, while Figure 6b and the top-view of the 3D velocity field for tests 15-19 (wave plus current). Within these tests the ADV positions follow the same cross pattern as tests 10-14, but with combined waves and current. Figure 6a shows that, in comparison with the

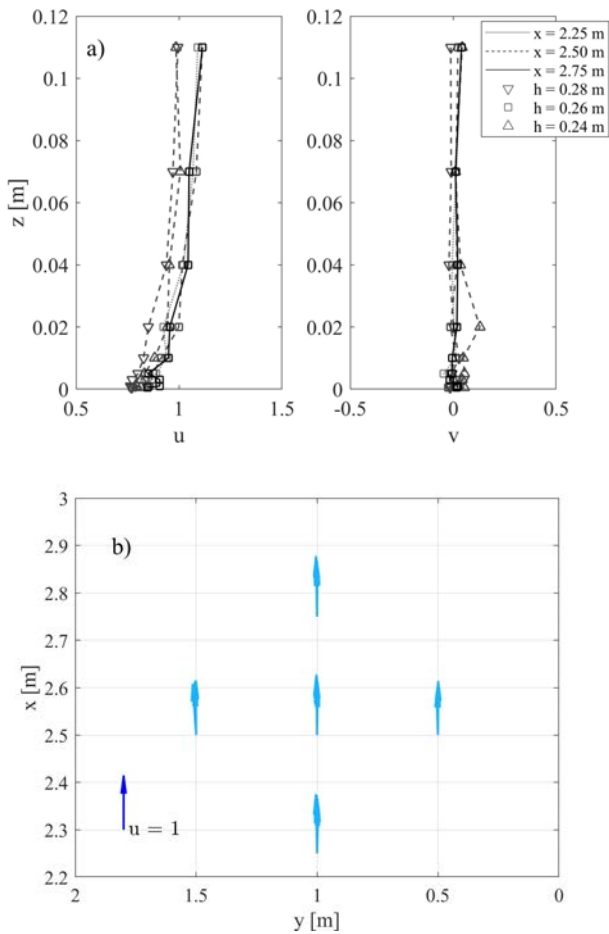


Fig. 5 - Dimensionless time-averaged velocity vertical profiles in the current direction (u) and in the wave direction (v) with different x (line) and y (markers) (a), and the top-view of the 3D velocity field (b) for tests 10-14 (current only). Local depth h ranges from 0.28 (test 10) m to 0.22 m (test 14).

current only case, u velocity profiles at the central and seaward positions present a velocity increase.

This suggests that the superimposed oscillatory flow determines a transfer of mean momentum to the flow in the current direction. This transfer is sufficiently large to reduce the current deviation in the shoreward direction determined by the recirculation region at the shoreward position. Moreover, profiles of v in Figure 6a show a mean flow in the seaward direction, which may be determined both by the recirculation effect and by the presence of a wave-generated undertow current determined by the presence of the sloping bed. Figure 6b shows, in comparison with the current only case shown in Figure 5b, the velocity increase observed in Figure 6a. Deviation of the flow is observed in the seaward direction in Figure 5a, at both seaward and shoreward positions, which confirms the presence of the undertow current.

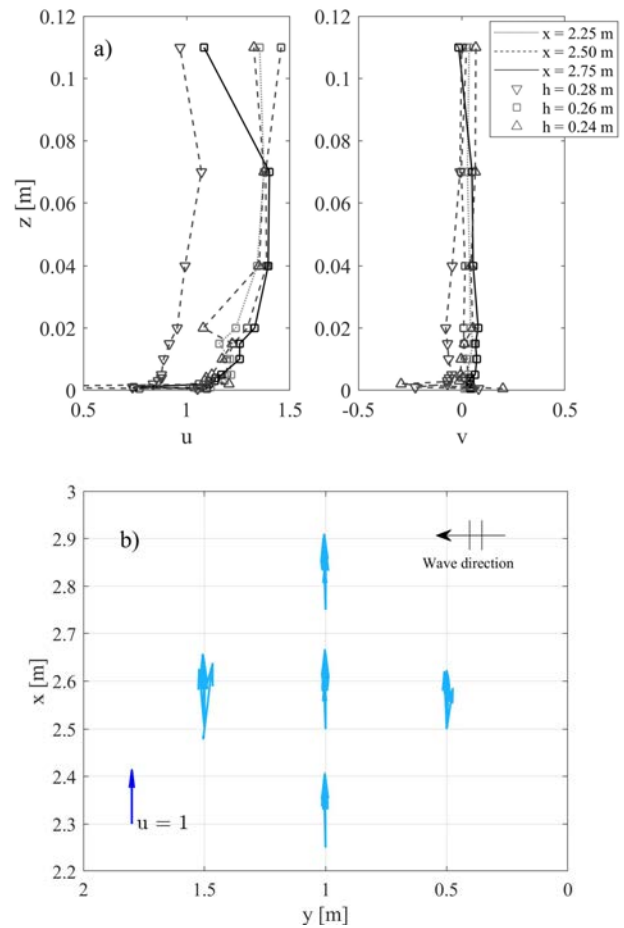


Fig. 6 - Dimensionless time-averaged velocity vertical profiles in the current direction (u) and in the wave direction (v) with different x (line) and y (markers) (a) and the top-view of the 3D velocity field (b) for tests 15-19 (wave plus current). Local depth h ranges from 0.28 (test 15) m to 0.22 m (test 19). Wave height $H = 0.01$ m, $T = 1.0$ s.

CONCLUSIONS

In the present work an experimental investigation on wave-current combined flow interacting at a right angle over a sloping planar beach has been carried out. The work aimed at investigating the complex interaction between wave and current over a varying water depth. Here the focus is on the hydrodynamic characterization of the experimental setup. This is fundamental to correctly interpret the experimental data.

Experiments have been conducted in a wave-current tank, where an oscillatory motion is generated by a wavemaker and it is superimposed to a steady current generated at a right angle with respect to the wave direction of propagation.

Surface elevation and 3D velocities have been recovered by means of 5 resistive wave gauges and an Acoustic Doppler Velocimeter. Experiments have been carried out in both current

only and wave plus current conditions. Results for current only tests showed that a satisfactory unidirectional steady current is achieved in the experimental tank. A recirculation phenomenon arises farther from the central axis of the inflow/outflow section, determining the flow to be directed along or opposite to the wave direction. Superposition of waves determined a velocity increase of the current, which suggests a transfer of mean momentum from the wave motion to the steady current. The transfer of momentum is sufficient to oppose the recirculation effect in the shoreward direction. Veering in the y direction opposite to the direction of waves suggest the presence of an undertow triggered by the presence of the slope.

The presented experimental setup is a promising device that can properly generate an oscillatory motion superimposed to an orthogonal steady current over a plane beach. Further

investigations should focus on: (i) the current turbulent field and how this is altered by the presence of wave motion; (ii) how to deal with or to reduce recirculation effects; (iii) shoaling effects and presence of nonlinear components and how they affect the steady current.

ACKNOWLEDGEMENTS

This work has been partly funded by the EU funded project HYDRALAB PLUS (proposal number 654110), by the project “news - Nearshore hazard monitoring and EarlyWarning System” (code C1-3.2-60) in the framework of the programme INTERREG V-A Italia Malta 2014-2020, by University of Catania funded projects “Interazione onde correnti nella regione costiera (inocs)”, “Piano triennale della Ricerca 2016-18” and by POR SICILIA FSE (CCI: 2014IT05SFOP014).

REFERENCES

- DE SERIO F. & MOSSA M. (2013) - *A laboratory study of irregular shoaling waves*. Experiments in fluids, **54** (6): 1536.
- DEAN R. G. (1970) - *Relative Validity of water Wave Theories*. J. Waterways Harbors Div., ASCE, **96** No. WW1: 105 - 119.
- FARACI C., SCANDURA P., MUSUMECI R. E. & FOTI E. (2018) - *Waves plus currents crossing at a right angle: near-bed velocity statistics*. Journal of Hydraulic Research, 1686, 1–18. <https://doi.org/10.1080/00221686.2017.1397557>.
- FARACI C., SCANDURA P. & FOTI E. (2015) - *Reflection of sea waves by combined caissons*. Journal of Waterway, Port, Coastal, and Ocean Engineering, **141**: 1 - 12. [https://doi.org/10.1061/\(ASCE\)WW.1943-5460.0000275](https://doi.org/10.1061/(ASCE)WW.1943-5460.0000275).
- FERNANDO P. C., GUO J. & LIN P. (2011) - *Wave-current interaction at an angle 2: Theory*. Journal of Hydraulic Research, **49** (4): 424 - 436. <https://doi.org/10.1080/00221686.2010.547036>.
- FERNANDO P. C., GUO J. & LIN P. (2011) - *Wave-current interaction at an angle 1: Experiment*. Journal of Hydraulic Research, **49** (4): 424 - 436. <https://doi.org/10.1080/00221686.2010.547036>.
- GORING D. G., & NIKORA V. I. (2002) - *Despiking Acoustic Doppler Velocimeter Data*. **128**: 117 - 126.
- GRANT W. D. & MADSEN O. S. (1979) - *Combined wave and current interaction with a rough bottom*. Journal of Geophysical Research: Oceans, **84** (C4): 1797 - 1808. <https://doi.org/10.1029/JC084iC04p01797>.
- KEMP P. H. & SIMONS R. R. (1983) - *The interaction of waves and a turbulent current: waves propagating against the current*. Journal of fluid mechanics, **130**: 73 - 89.
- LIM K. Y. & MADSEN O. S. (2016) - *An experimental study on near-orthogonal wave-current interaction over smooth and uniform fixed roughness beds*. Coastal Engineering, **116**: 258 - 274. <https://doi.org/10.1016/j.coastaleng.2016.05.005>.
- LODAHL C. R., SUMER B. M. & FREDSOE, J. (1998) - *Turbulent combined oscillatory flow and current in a pipe*. Journal of Fluid Mechanics, **373**: 313 - 348. <https://doi.org/10.1017/S0022112098002559>.
- MARINO M., CÀCERES RABIONET, I., MUSUMECI R. E. & FOTI E., (2018) - *Reliability of pressure sensors to measure wave height in the shoaling region*. Proceedings of the 36th International Conference on Coastal Engineering, ICCE 2018; Baltimore; United States; 30 July 2018 through 3 August 2018; Code 152266. DOI: 10.9753/icce.v36.papers.10.
- MARINO M., MUSUMECI R. E. & FARACI C., (2020) - *Shoaling waves interacting with an orthogonal current*. Journal of Marine Science and Engineering, **8** (4), 281. <https://doi.org/10.3390/jmse8040281>.
- MATHISEN P. P. & MADSEN O. S. (1996) - *Waves and currents over a fixed rippled bed 2*. Bottom and apparent roughness experienced by currents in the presence of waves. Journal of Geophysical Research: Oceans, **101**(C7): 16543 - 16550.
- MUSUMECI R. E., CAVALLARO L., FOTI E., SCANDURA P. & BLONDEAUX P. (2006) - *Waves plus currents crossing at a right angle: Experimental investigation*. Journal of Geophysical Research: Oceans, **111** (7). <https://doi.org/10.1029/2005JC002933>.
- MUSUMECI R. E., MARLETTA V., SANCHEZ-ARCILLA, A. & FOTI E. (2018) - *A ferrofluid-based sensor to measure bottom shear stresses under currents and waves*. Journal of Hydraulic Research, **56** (5): 630 - 647. doi:10.1080/00221686.2017.1397779.
- SANCHO F., MENDES, P. A., CARMO J. A., NEVES M. G., TOMASICCHIO G. R., ARCHETTI R., DAMIANI L., MOSSA M., RINALDI, A., GIRONELLA X. & SANCHEZ-ARCILLA A. (2002) - *Wave hydrodynamics over a barred beach*. In Ocean Wave Measurement and Analysis, 1170 - 1179).
- SLEATH J. F. A. (1987). *Turbulent oscillatory flow over rough beds*. Journal of Fluid Mechanics, **182**: 369 - 409.

SVENDSEN I. A. (2006) - *Introduction to nearshore hydrodynamics* (24) World Scientific.

STANCANELLI L. M., MUSUMECI R. E. & FOTI E. (2018) - *Dynamics of gravity currents in the presence of surface waves*. Journal of Geophysical Research: Oceans, **123** (3): 2254 - 2273. doi:10.1002/2017JC013273.

STANCANELLI L. M., MUSUMECI R. E., STAGNITTI M. & FOTI E. (2020) - *Optical measurements of bottom shear stresses by means of ferrofluids*. Experiments in Fluids, **61** (2): 52.

VIVIANO A., MUSUMECI R. E. & FOTI E. (2018) - *Interaction between waves and gravity currents: Description of turbulence in a simple numerical model*. Environmental Fluid Mechanics, **18** (1): 117 - 148.

Received September 2019 - Accepted January 2020